Silicon isotope engineering for the development of better classical and quantum computers

Kohei Itoh
Keio University, Yokohama Japan
Kitoh@appi.keio.ac.jp

Contents

1. Silicon semiconductor engineering
2. Better Si chips for classical computers
   - Highly thermal conductive silicon
   - Probing thermal oxidation mechanism
   - Probing Si diffusion during heat processing
3. Superconductivity in Ba_8Si_{46} clathrate
4. All silicon quantum computers
   ^{29}Si nuclear spins embedded in spin-free ^{28}Si matrix

Collaborators

Isotope engineering:	Eugene E. Haller (UC Berkeley)
	Hans- J. Pohl (U. Jena)
Oxidation studies:	Tomonori Takahashi (Keio University)
	Shigeto Fukatsu (Keio University)
	Masashi Uematsu (NTT Basic Research Lab)
	Hiroyuki Kageshima (NTT Basic Research Lab)
	Yasuo Takahashi (NTT Basic Research Lab)
	Kenji Shiraishi (University of Tsukuba)
Ba_8Si_{46} clathrate	Tomoko Shimizu (Keio University)
	Katsumi Tanigaki (Osaka City University)
Si quantum computers	Eisuke Abe (Keio University)
	Ryusuke Nebashi (Keio University)
	Yoshinori Matsumoto (Keio University)
	Hideo Ohno (Tohoku University)
	Yuzo Ohno (Tohoku University)
	Susumu Sasaki (Nigata University)
	Yoshhisa Yamamoto (Stanford University)
	Thaddeus Ladd (Stanford University)
	Jonathan Goldman (Stanford University)
	Fumiko Yamaguchi (Stanford University)
	Anne Verhulst (Stanford University)

1. Semiconductor Isotope Engineering

List of stable isotopes

^{28}Si 92.2%

^{29}Si 4.7% → 1/2 (nuclear spin)

^{30}Si 3.1%

^{70}Ge 20.5%

^{72}Ge 27.4%

^{73}Ge 7.8% → 9/2 (nuclear spin)

^{74}Ge 36.5%

^{76}Ge 7.8%

^{69}Ga 60.1% → 3/2

^{71}Ga 39.9% → 3/2 (nuclear spin)

^{75}As 100% → 3/2

Mass and nuclear spin Control through manipulation of stable isotopes

Si bulk crystal growth

Floating-zone Si grower

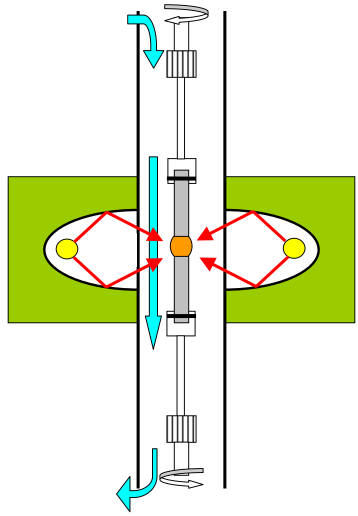

Isotopically controlled Si fabrication

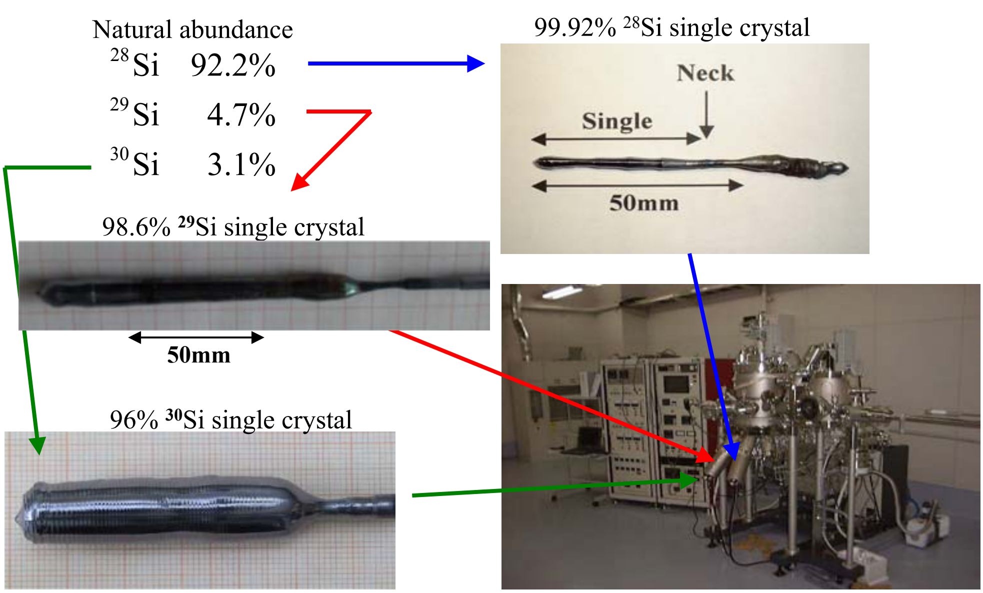

2. Better Si chips for classical computers

MOSFET

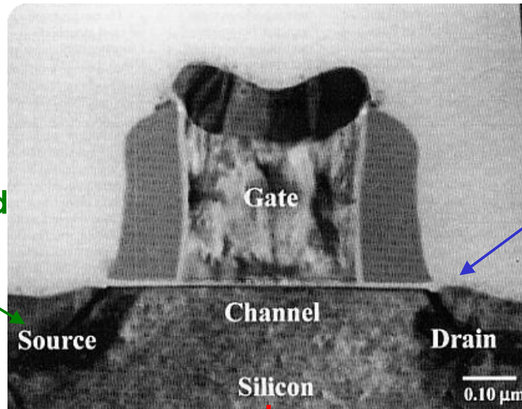

3. Impurity and Si diffusion

2. SiO_2 formation

1. Heat flow

Isotope effect on thermal conductivity of Si

Thermal conductivity of 99.86% ^{28}Si

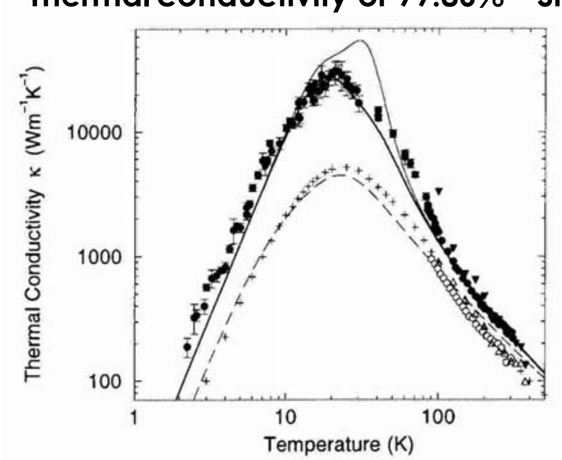

300K 60% increase

400K 40-50% increase

with respect to natural Si

T. Ruf, *et al.* Solid State Commun. 2000

Temperatures in a 1GHz microprocessor (simulation)

Temperatures in Celsius for

an isotopically enriched ^{28}Si substrates and

a natural Si substrate in parentheses

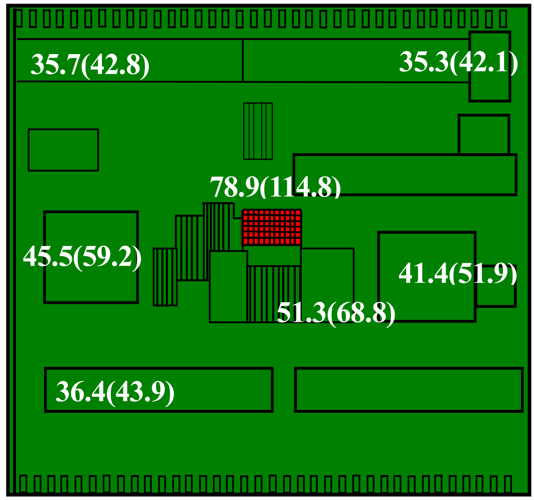

Thermal conductivity enhancement

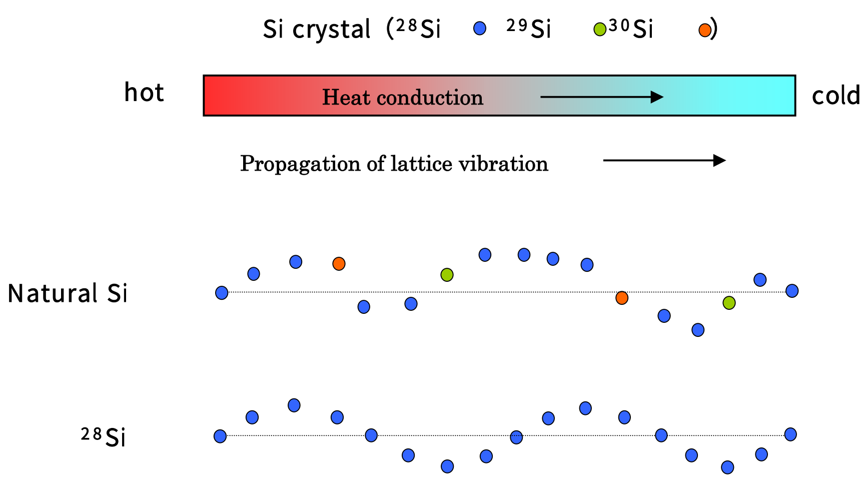

Comparison with theory

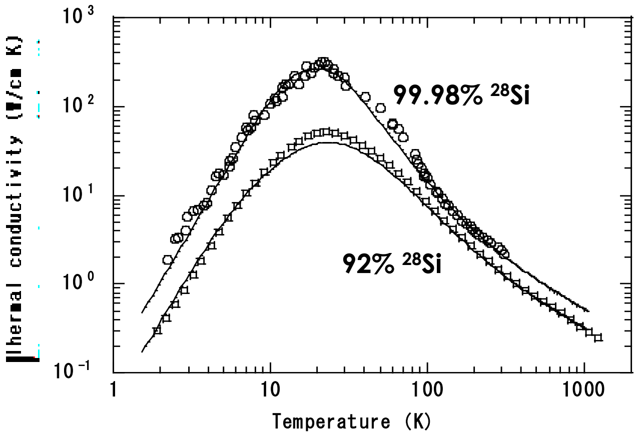

1. Isotope scattering

$$g = \frac{\sum c_i M_i^2 - \left(\sum c_i M_i\right)^2}{\left(\sum c_i M_i\right)^2}$$

2. Boundary scattering
3. Normal process (phonon)
4. Umklapp process (phonon)

Fit based on M. G. Holland: Phys. Rev. **132** (1963) 2461

Thermal oxidation of Si

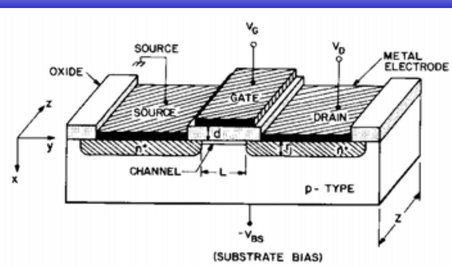

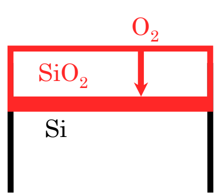

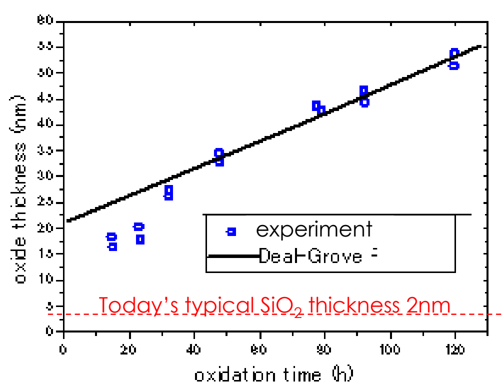

Deal and Grove's model

J.Appl.Phys.,**36**.3770(1965)

Does Si diffuse into SiO_2 ?

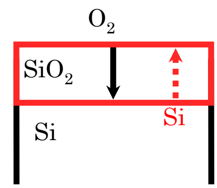

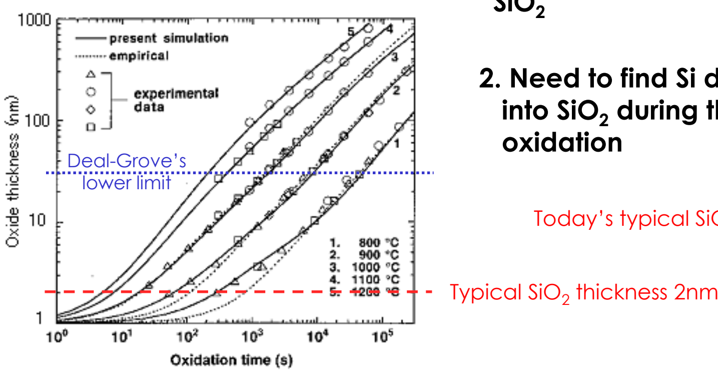

M. Uematsu et al. Jpn. J. Appl. Phys. **39** (2000) L699

1. Need to know Si diffusion coefficient in thermally grown SiO_2

2. Need to find Si diffusing into SiO_2 during thermal oxidation

Today's typical SiO_2 thickness 2nm

Self-Diffusion of Si in SiO_2

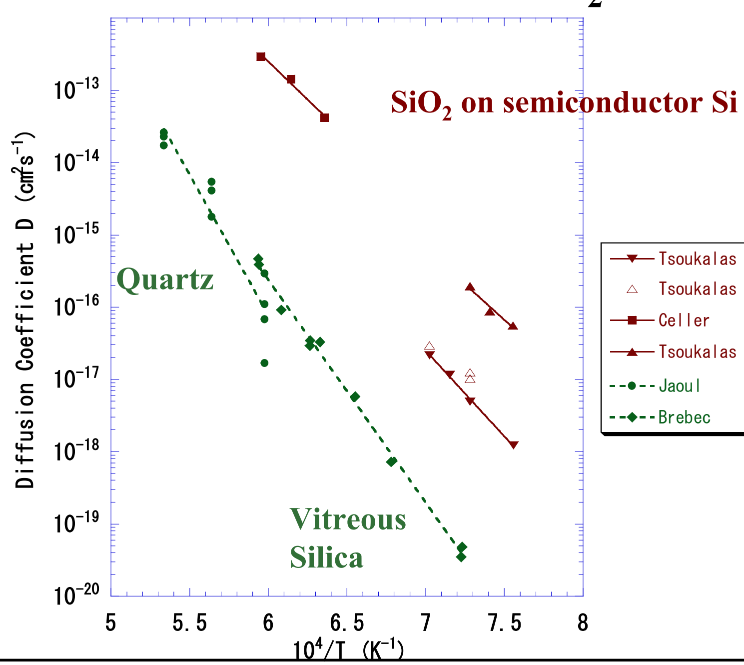

Diffusion studies with stable isotopes

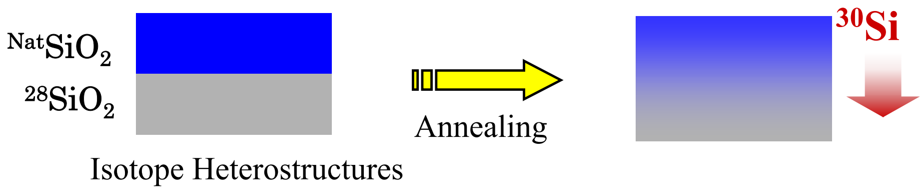

Diffusion of ^{30}Si ⇒ SIMS Measurement

Isotope Composition of $^{Nat}SiO_2$ and $^{28}SiO_2$

Isotope	^{28}Si	^{29}Si	^{30}Si
$^{Nat}SiO_2$	92.2%	4.7%	3.1%
$^{28}SiO_2$	99.924%	0.073%	0.003%

Preparation of Samples

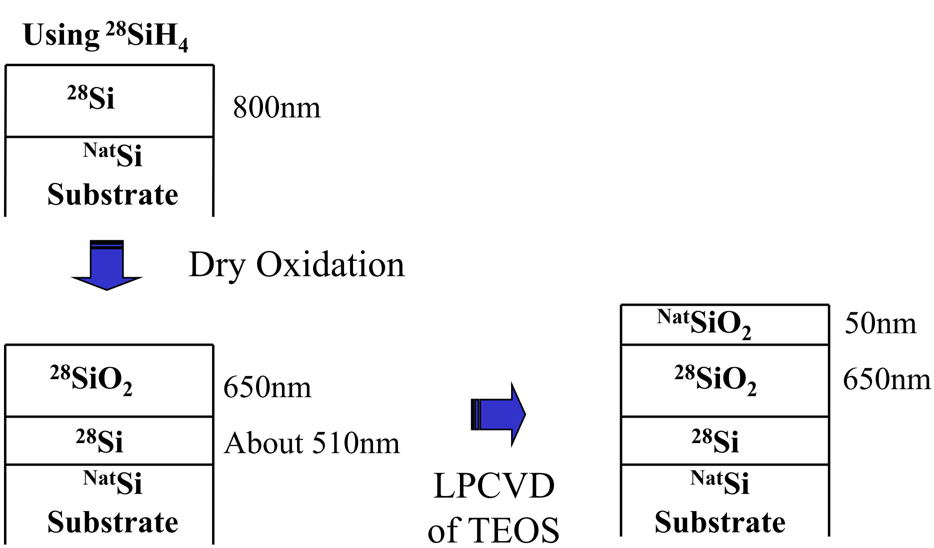

Annealing

- 1150,1200,1250,1300℃
- Flowing Ar+1%O_2

  Oxygen prevents decomposition of SiO_2

  Concentration of oxygen Low → Decomposition High → Oxidation

- Flowing Ar+20% O_2

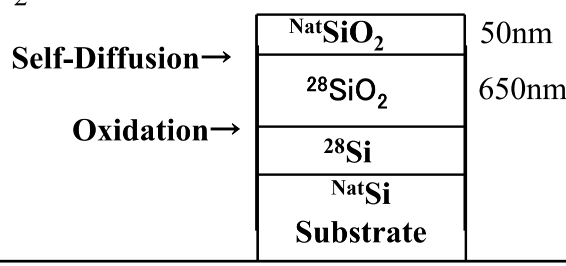

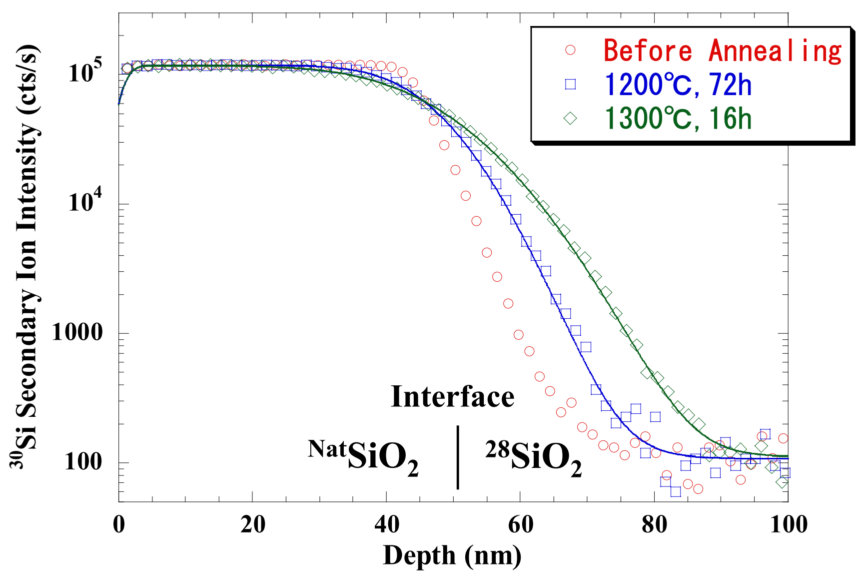

Diffusion Profile of ^{30}Si

$$C(x) = C_{28} + \frac{C_{Nat} - C_{28}}{2}\left[erf\left(\frac{x+h}{2\sqrt{Dt}}\right) - erf\left(\frac{x-h}{2\sqrt{Dt}}\right)\right]$$

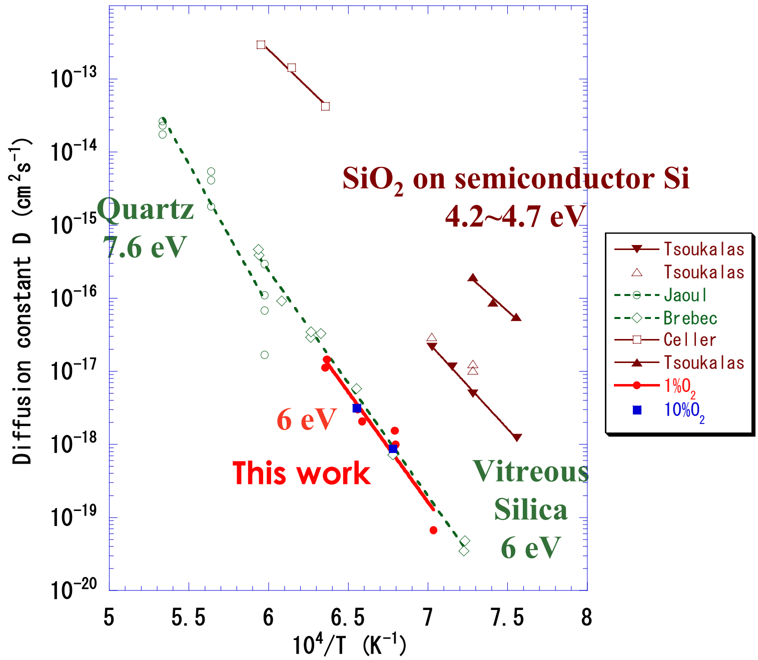

Direct observation of Si diffusion into SiO_2

I. MBE growth of ^{28}Si

II. Thermal oxidation

III. Depth profile by secondary ion mass spectrometry (SIMS)

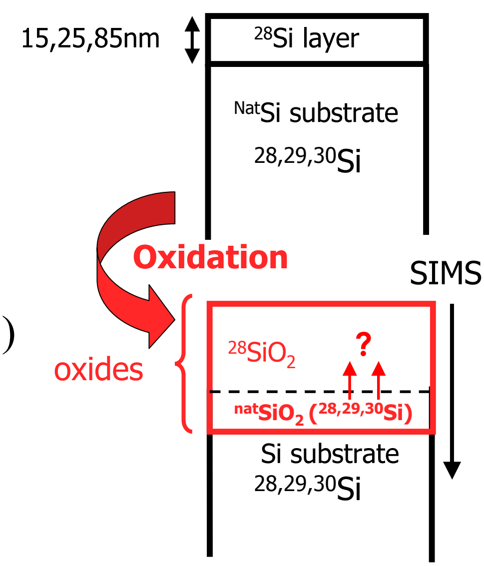

SIMS measurements

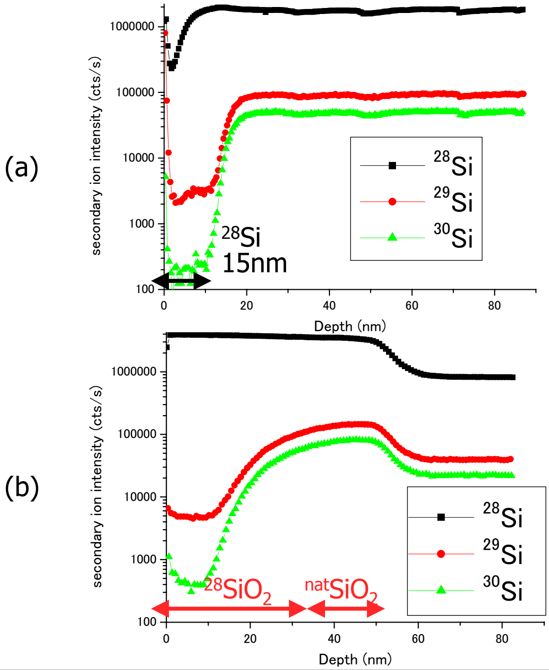

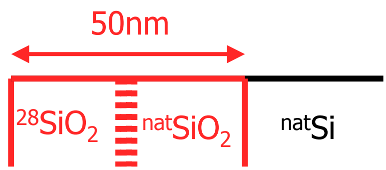

Fig. 8 SIMS profile
(a)as grown (b)1000℃,60min

Oxidation for nano-scale fabrication

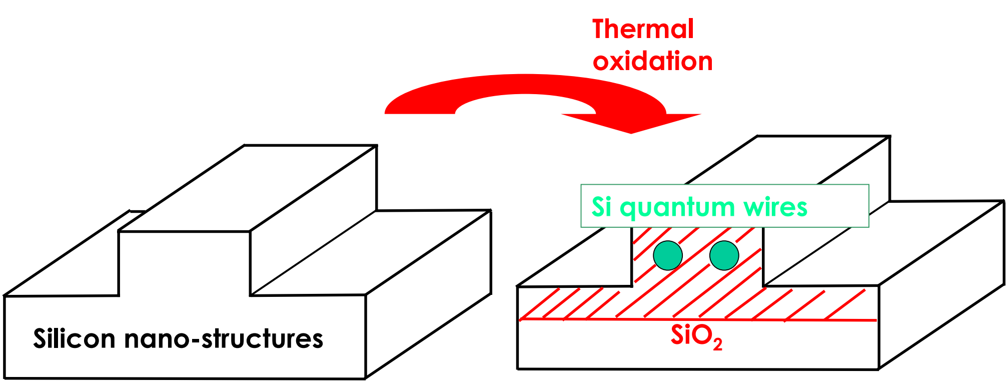

Impurity and Si diffusion

MOSFET

Impurity and Si diffusion

^{28}Si layer

^{30}Si layer

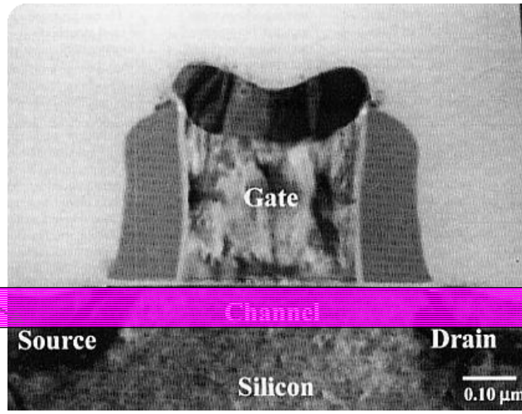

3. Superconductivity in Ba_8Si_{46} clathrate

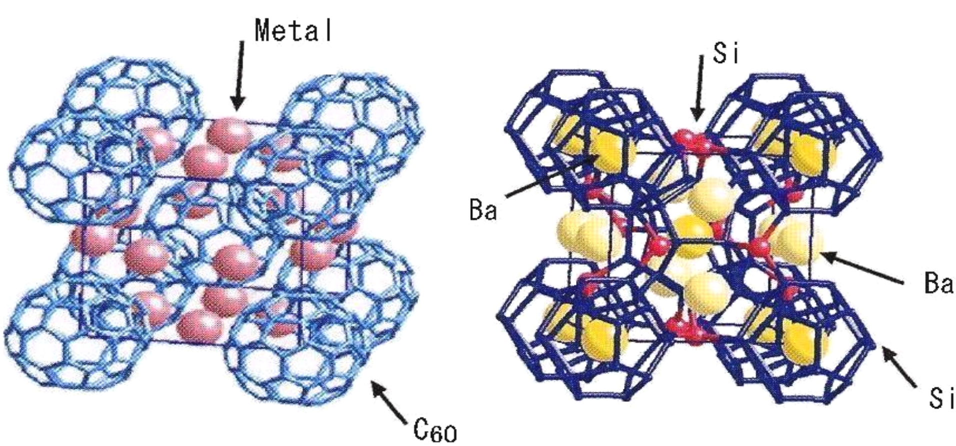

(a) M_xC_{60} (b) Ba_8Si_{46}

Structure of Group Ⅳ Clusters

Superconductor Ba_8Si_{46}

Ba doped Si_{46} Clathrate

↑

High Pressure Synthesis

Critical Temperature
Tc＝8K

- Lattice const. ↑ by Ba doping
- Strong hybridization between Si_{46} band and Ba orbital

→ $N(E_F)$ becomes large

S.Yamanaka et al. “High-Pressure Synthesis of a New Silicon Clathrate Superconductor, Ba_8Si_{46}” Inorg. Chem. 39 (2000) 56

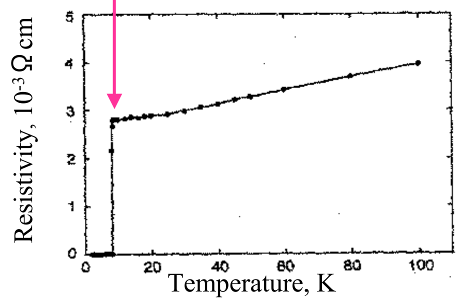

Temperature dependence of the resistivity of Ba_8Si_{46}

BCS model

$$T_c = 1.14\frac{\hbar\omega}{k_B}\exp\left(-\frac{1}{N(E_F)V}\right) \propto \omega \qquad \omega = \sqrt{\frac{k}{m}}$$

Density of states at the Fermi Level High (55states/eV)	e^--phonon Interaction ?	Phonon frequency

→ check for the isotope effect (^{28}Si and ^{30}Si)

Isotope effect on T_C

From BCS Theory

$Tc(^{30}Si)/Tc(^{28}Si)$

$= \sqrt{28}/\sqrt{30}$

$= 0.97$

From Experimental Result

$Tc(Ba_8{}^{30}Si_{46})/Tc(Ba_8{}^{28}Si_{46})$

$= 8.02K/8.07K$

$= 0.99$

BCS-like

Osaka city university, Tanigaki group

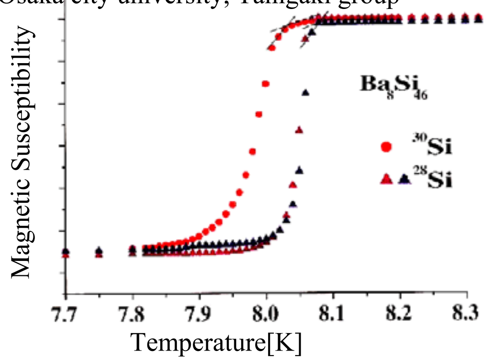

Temperature dependence of Magnetic Susceptibility of $Ba_8{}^{28}Si_{46}$ and $Ba_8{}^{30}Si_{46}$

Raman studies of vibrational modes

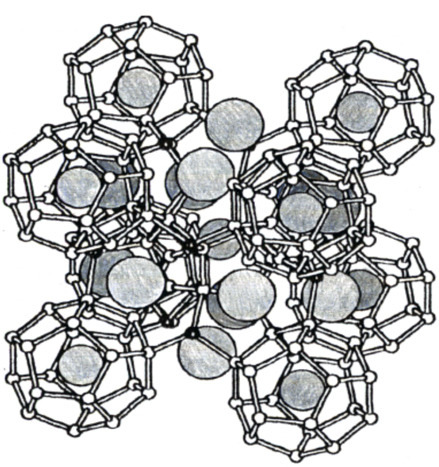

Ba_8Si_{46} { Si-Si, Si-Ba, Ba-Ba

Raman results

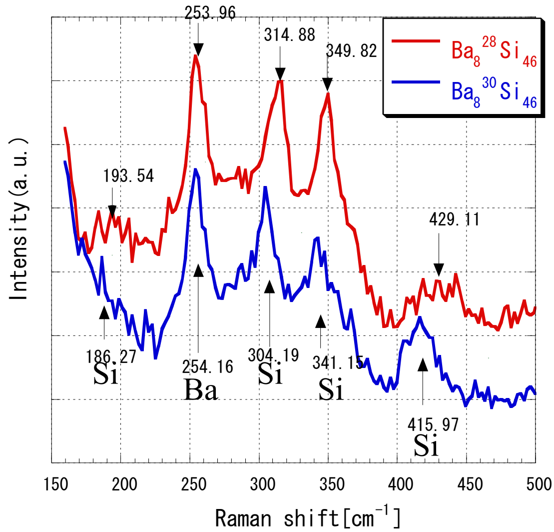

Raman spectra of $Ba_8{}^{28}Si_{46}$ and $Ba_8{}^{30}Si_{46}$

5 peaks observed

- 4 shifted
  - → Si-related modes
  - wavenumber ratio
  - k(30)/k(28) = 0.96～0.98
  - mass ratio
  - $\sqrt{28}/\sqrt{30} = 0.97$
- 1 does not shift
  - → Ba related

Raman results

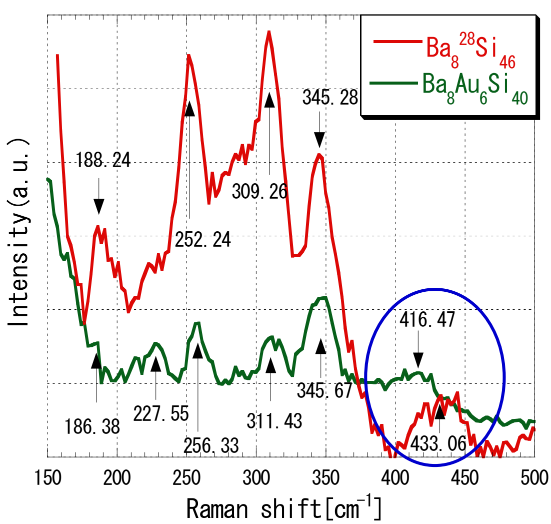

Raman spectra of $Ba_8{}^{28}Si_{46}$ and $Ba_8Au_6Si_{40}$

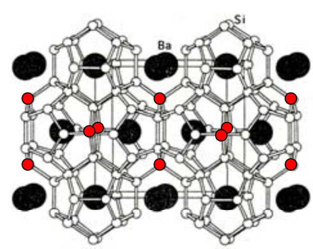

● : c-site Si or Au

Fermi surface related site

430cm^{-1} peak is related to Si at c-sites

Quantum computation with spins

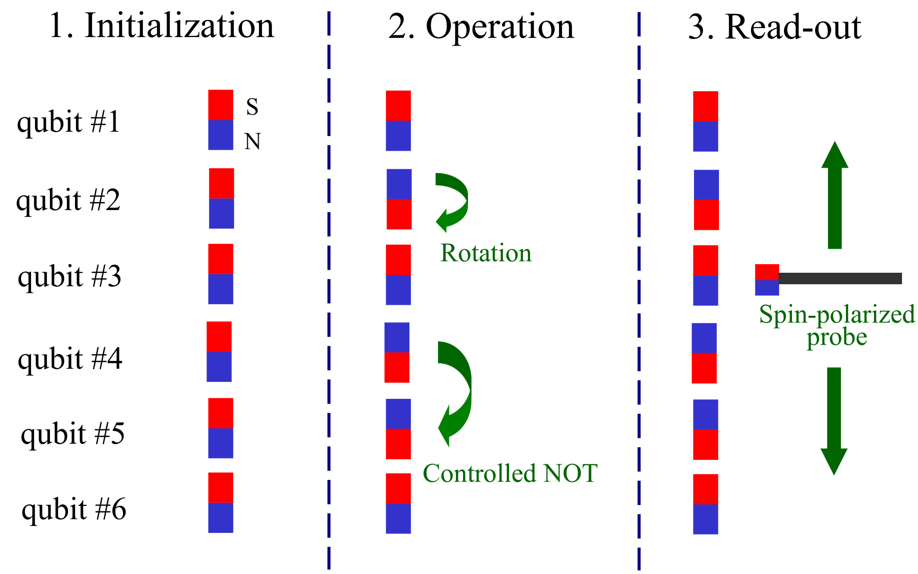

Figure of merits for QC

1. **Number of qubits: n**

   available number of states 2^n

2. **Maximum total computable steps: N_{max}**

$$N_{max} = \frac{\text{phase decoherence time: } T_2}{\text{time needed for each operation: } t_s}$$

Solution NMR Quantum Computation

4. Measurement is facilitated by huge ensemble of independent copies

1. A small number of stable qubits provided by distinct spin 1/2 nuclei

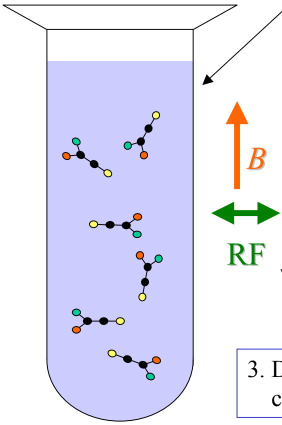

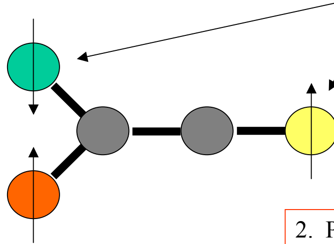

5. Decoherence times are long since nuclei interact only weakly with environment

2. Perfect initialization is not possible. Instead, "pseudo-pure" states must be used

3. Dipolar interactions controllable by RF

N. A. Gershenfeld and I. Chuang, *Science* **275**, 350 (1997)
D. G. Cory, A. F. Fahmy, and T. F. Havel, *Proc. Natl. Acad. Sci. USA* **94**, 1634 (1997)

Solid-State Impurity NMR QC

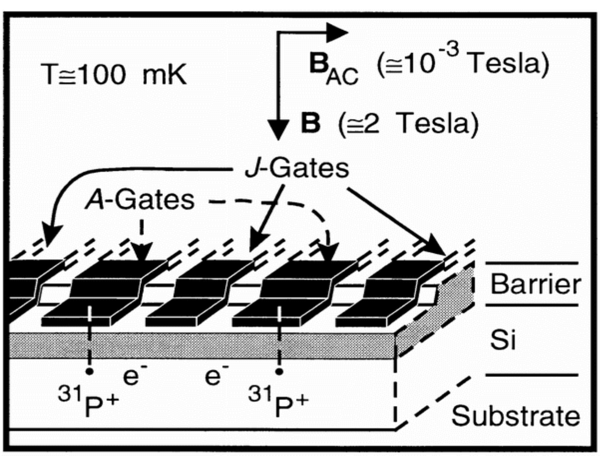

B. E. Kane, *Nature* **393**, 133 (1998)

1. Isolated impurity nuclei provide qubits
2. Low temperature electrons allow initialization
3. Electron-mediated interactions controlled by gates
4. Single-spin measurement via nuclear-electron coupling is proposed
5. Well-separated impurities have long decoherence times

Motivation

Solution NMR QC

N. A. Gershenfeld and I. Chuang, *Science* **275**, 350 (1997)
D. G. Cory, A. F. Fahmy, and T. F. Havel, *Proc. Natl. Acad. Sci. USA* **94**, 1634 (1997)

Advantages:
- Ensemble measurement
- Natural (chemical) fabrication

Disadvantages:
- Challenging to scale to many qubits and/or gates
- Initialization difficult

Solid-State Impurity QC

B. E. Kane, *Nature* **393**, 133 (1998)
R. Vrijen, *et al., Phys. Rev. A* **62,** 012306 (2000)
G.P. Berman, G. D. Doolen, P. C. Hammel, and V. I. Tsifrinovich, *Phys. Rev. B* **61**, 14694 (2000).

Advantages:
- Scalable!
- Can cool to low temperatures for initialization

Disadvantages:
- Need single-spin measurement
- Challenging fabrication

All Silicon QC uses advantages of both!

^{29}Si nuclear spin quantum computer

Qubit #1 ω_1

Qubit #2 ω_2

Qubit #3 ω_3

Qubit #4 ω_4

$|\omega_{n+1} - \omega_1| \sim 20$kHz

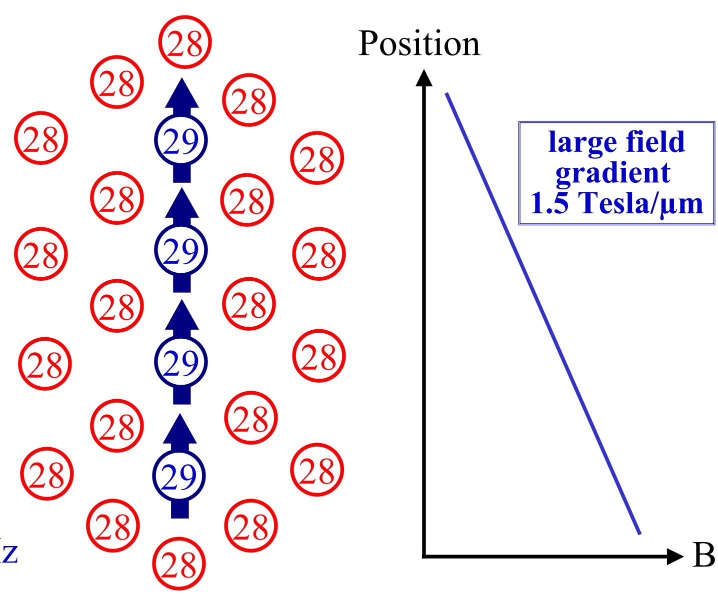

Magnetic Resonance Force Microscopy

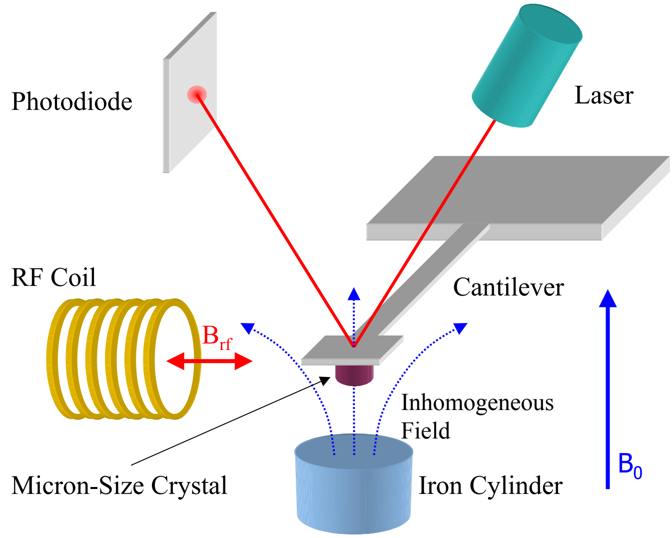

The ferro-/para-/nuclear magnetic sample feels the force:

$$F^z(t) = m_z(t)\frac{\partial B^z}{\partial z}$$

, which makes the cantilever oscillate

An all silicon quantum computer

- ***Qubits are spin-1/2 ^{29}Si nuclei in a ^{28}Si crystal***. They are distinguished by a one-dimensional ***field gradient***.
- Initialization is accomplished by cooling, optical pumping, "boosting," and "pseudo-pure state" techniques.
- Qubit interactions (***decoupling and recoupling***) are accomplished with RF pulse sequences.
- An ensemble of copies, orthogonal to the gradient direction, allow measurement by ***MRFM***.
- Decoherence times are limited by pulse sequence design, crystal purity, and cantilever stability.

^{29}Si wires embedded in the ^{28}Si matrix

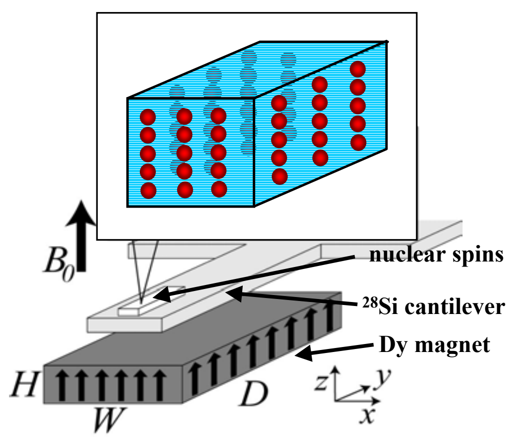

Improvement of Ladd, Goldman, Yamaguchi and Yamamoto, quant-ph/0009122 (2001)

Alternative configuration

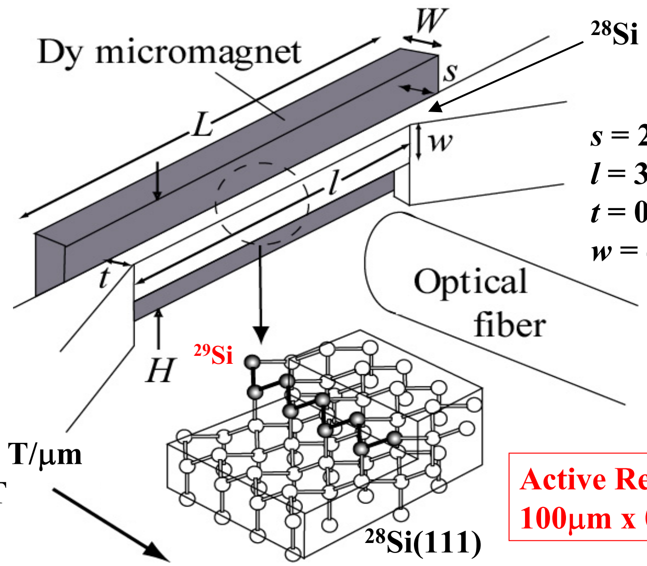

L = 400 μm
W = 4 μm
H = 10 μm

s = 2.1 μm
l = 300 μm
t = 0.25 μm
w = 4 μm

dB^z/dz = 1.4 T/μm
B_0 = 7 T

Active Region:
100μm x 0.2μm

^{29}Si wire fabrication

- Form regular step arrays on slightly miscut ^{28}Si(111)7×7 surface (~ 1° from normal)
- Steps are *straight*, with about 1 kink in 20000 sites.
- ^{29}Si chains formed by "Step Decoration" from ^{28}Si steps
- Angle of miscut controls chain spacing

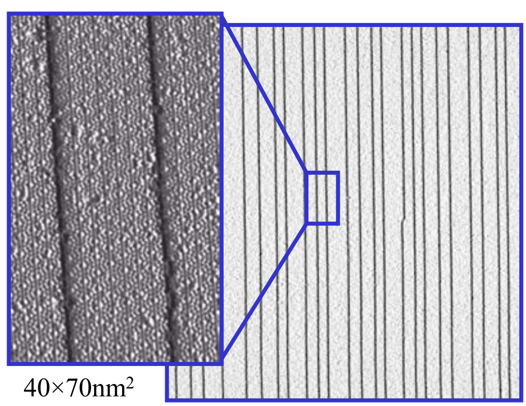

40×70nm^2

340×390nm^2

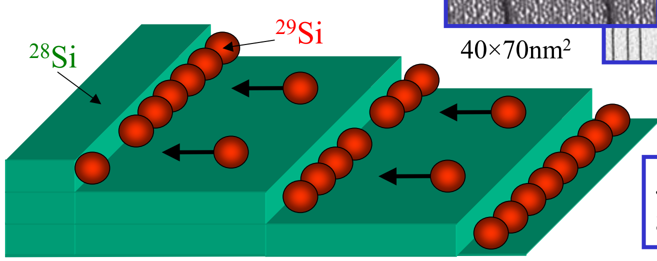

J.-L. Lin, *et al.*, *JAP* **84**, 255 (1998)

MBE fabrication of ^{29}Si wire copies

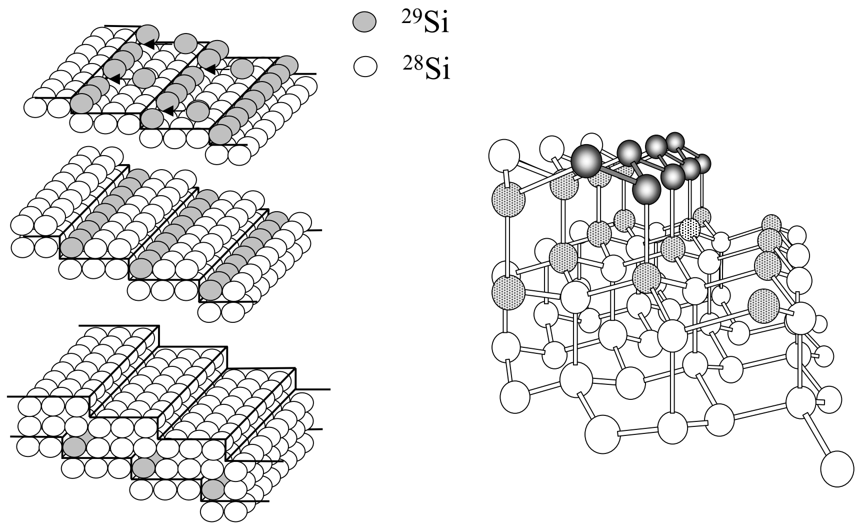

Polarization by optical pumping

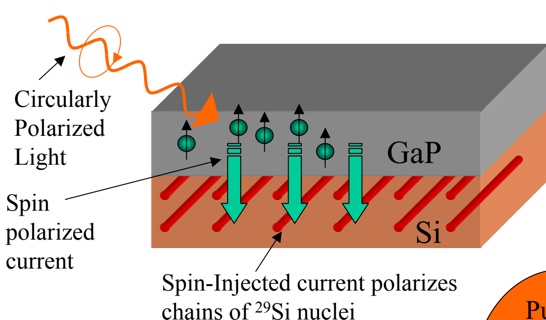

The spin-polarized conduction electrons are cleared away after polarization, removing them as decoherence source

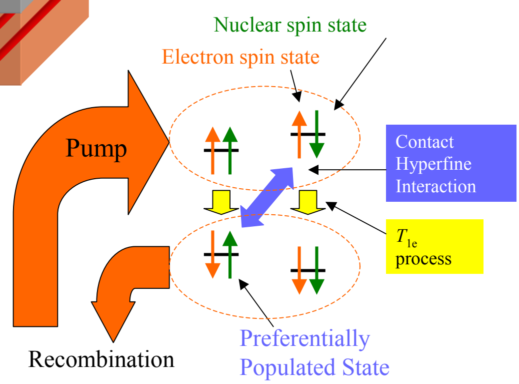

G. Lampel, *Phys. Rev. Lett.* **20,** 491 (1967)
R. Tycko, *Solid State Nuclear Magnetic Resonance* **11,** 1 (1998)

Operation (decoupling)

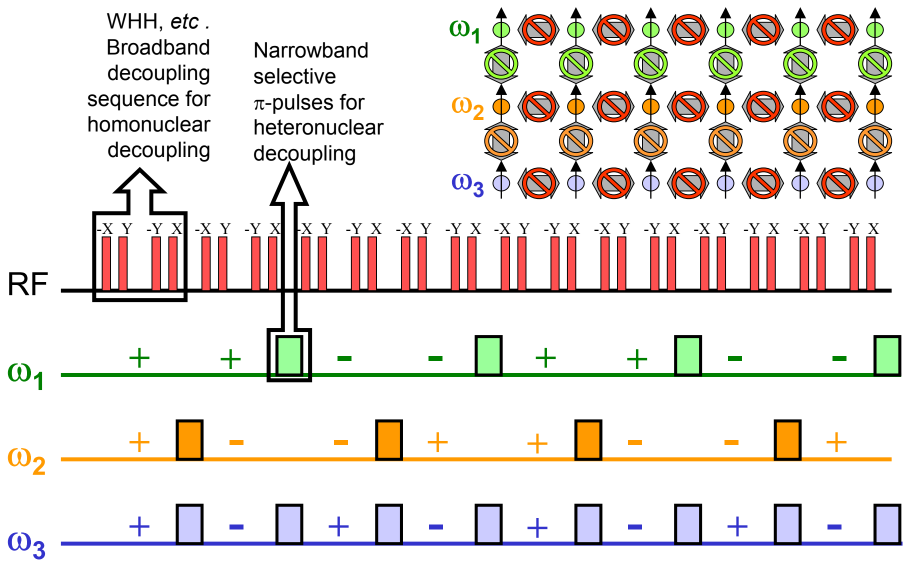

Operation (recoupling)

D. W. Leung, I. Chuang, F. Yamaguchi and Y. Yamamoto, Phys. Rev. A, 61(4) 042310/1 (1999)

- Qubits may be selectively recoupled
- Add single spin rotations to make controlled-NOT

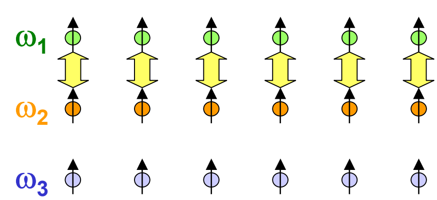

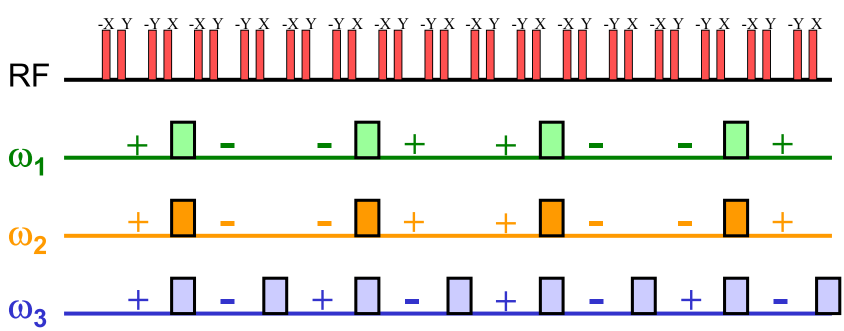

Read-out by the MRFM cantilever

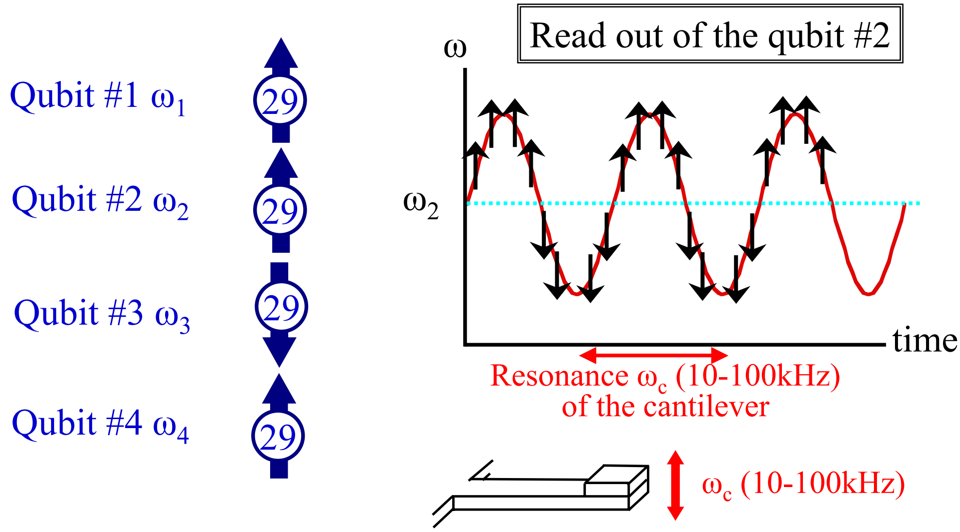

SNR and number of qubits

Force resolution for a cantilever in the thermal limit:

$$F_{\min} = \sqrt{4kk_B TB/\omega_0 Q}$$

Force generated from a single atomic plane:

$$F(t) = M_z(r,t)\frac{\partial B_z}{\partial z}$$

Magnetization for nuclear spins in plane:

$$M_z = \gamma \hbar IN\left[\left(\frac{1+P}{2}\right)^n - \left(\frac{1-P}{2}\right)^n\right]$$

Number of qubits (n) for SNR = 1 vs. nuclear polarization

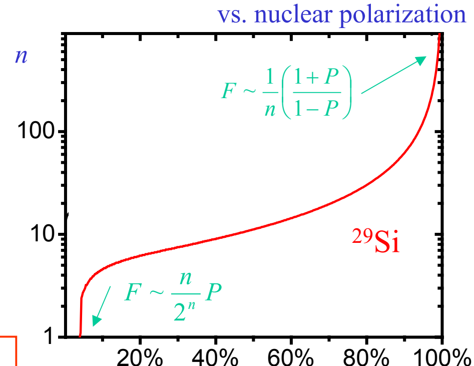

nuclear polarization (P)

N = number of qubit copies

n = number of qubits in QC

Decoherence and th emaximum operation step

$$\frac{1}{T_2} = \frac{1}{2T_1} + \frac{\gamma^2}{2}\int_{-\infty}^{\infty}\langle \partial B_Z(t)\partial B_Z(0)\rangle dt + \left(\langle [H_{\mathrm{dip}}^{\mathrm{res}}, [H_{\mathrm{dip}}^{\mathrm{res}}, I^x]]\rangle / \langle I^x \rangle\right)^{1/2}$$

DC spectral density of local fluctuating field

Second Moment due to residual dipolar couplings

Primary Decoherence Sources:

Residual Dipolar Couplings
- Reversible in principle
- Present sequence: $T_2 \sim 10$ ms

Cantilever Drift
- Thermal equilibrium: $T_2 \sim 200$ ms
- Feedback control $\Rightarrow T_2 \sim 1$ hour

Paramagnetic Impurites
- Assuming very dilute impurities, $T_2 \sim (\omega_0 T_{1e})^{-1/2} T_1 \sim 1$ minute, but much shorter for nuclei near impurity

Clock period $t_c = Ln^2/\Delta\omega$ set by pulse sequence.
$\Rightarrow$ Number of logic gates T_2/t_c is limited

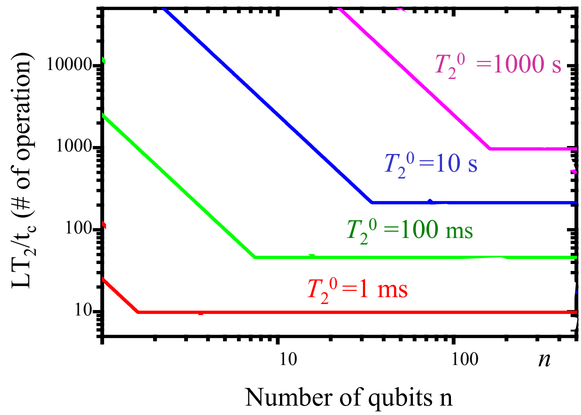

Step by step

Step.1 for Cantilever Fabrication & MRFM Readout

Few-hundred-nanometer-thick ^{29}Si on natural Si substrate

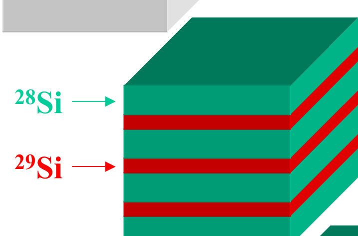

Step.2 toward Quantum Computation

$(^{29}Si)_n / (^{28}Si)_m$ isotope silicon superlattices with various n & m

Step.3 for First Logic Gates

Two single-layer of ^{29}Si as qubits

Our estimate allows a few logic gates in particular configurations, which are barely enough for *"proof of principle"*

Why ^{29}Si in ^{28}Si

- **Established crystal growth, processing and isotope engineering technologies**
- **Longest possible decoherence time**
  No extrinsic electron and nuclear spins, reduced magnetic impurities
- **Minimum cross-talk between qubit copies but enough ensemble of qubit copies**
- **^{28}Si matrix provides natural means for optical pumping and detection of ^{29}Si nuclear spins**
- **Highest-possible-Q magnetic resonance force microscope (MRFM) cantilever**
- **Possible integration with Si CMOS and SET circuits**